Journal of Colloid and Interface Science **224,** 76–83 (2000)
doi:10.1006/jcis.1999.6673, available online at http://www.idealibrary.com on IDEAL®

Adsorption of Water-Soluble Proteins onto Bubbles in Continuous Foam Separation

Hideo Maruyama,[1] Akira Suzuki, and Hideshi Seki

Department of Marine Bioresources Chemistry, Faculty of Fisheries, Hokkaido University, Minato-cho 3-1-1, Hakodate, Hokkaido 041-8611, Japan

E-mail: maruyama@elsie.fish.hokudai.ac.jp

Received April 5, 1999; accepted December 13, 1999

The mechanism of water-soluble protein enrichment in continuous foam separation was studied. The liquid flow rate and the protein concentration in the foam phase were measured at various heights from the interface between the bulk liquid and foam layer, and the intrinsic values at the interface were estimated by the extrapolation method to determine the accurate adsorption density on the bubble surface. Ovalbumin (OA) and hemoglobin (HB) were used as the soluble proteins. The solution pH values were varied from 3.5 to 6.0 for OA and from 6.0 to 8.0 for HB. The experimental isotherms for OA and HB were compared to the Langmuir isotherm, and the two adsorption parameters of the equilibrium constant, K, and the saturated density, γ, at each pH were determined. Both γ values obtained for OA and HB showed maxima at their isoelectric point (pH 4.6 for OA and pH 6.8 for HB). Assuming that OA and HB molecules are spherical in shape and are adsorbed on the bubble surface in a close-packed structure at saturation, the calculated diameters for OA and HB molecules were quite similar to the literature values. The variation in γ for both OA and HB is discussed qualitatively in relation to the net charge of the protein molecule.
© 2000 Academic Press

Key Words: **foam separation; adsorption; protein enrichment; liquid–foam interface; ovalbumin; hemoglobin.**

INTRODUCTION

The foam separation technique has been widely used in ore flotation (1), waste water treatment (2), and so on. Recently, it appears that the separation of proteins by this method has been studied on the basis of its possible applicability to food and biochemical industries (3–7). For the optimal design and operation of industrial processes, it is necessary to determine the adsorption and enriching mechanism of protein onto bubble surface in this technique.

The enriching process in foam separation technique is classified into two stages: (i) adsorption of the objective substance onto the bubble surface in a dispersed bubble bed, and (ii) enrichment in a foam bed due to coalescence of bubble cells and liquid drainage. The former is well characterized by the physicochemical properties of objective substance, which influence the adsorption density at bubble–liquid interface and the production rate of bubble–liquid interfacial area. Adsorption behavior of proteins on bubble surface must be clarified to apply this technique to these foam separation processes. However, there are few reports on adsorption behavior of soluble proteins in the foam separation method. The latter is common in all foam separations and would be a function of liquid properties, operating conditions, and liquid content in foam layer.

In previous studies about foam separation (8–14), the adsorption density, X, on bubble surfaces has often been determined from a relationship concerning an overhead concentration based on the mass balance of the foaming column by the relationship

$$X = (W_f/S_b)(C_f - C_b), \qquad [1]$$

where C_b, C_f, W_f, and S_b represent the bulk and collapsed foam liquid concentrations in equilibrium, the volumetric flow rate of liquid in foam (collapsed foam liquid), and the bubble–liquid interfacial area generation rate in the pool, respectively. The values of all terms in the right-hand side in Eq. [1] could be determined or estimated by some ways. However, it should be necessary to measure the flow rate of liquid in foam and to collect the collapsed foam liquid by keeping the foam height as near to the liquid–foam interface as possible, because the volumetric flow rate of liquid in foam decreases exponentially in the axial direction, and this decrease is much larger the higher the position of the foam within the column (15, 16). This fact suggests that the amount of the adsorbate contained in foam liquid should be distributed; moreover, the concentration of the liquid in the foam will change with the overflowing and the sampling position in the axial direction of the column. To determine the adsorption density on bubble surface in foam separation, the intrinsic values of volumetric flow rate and the protein concentration in foam would have to be determined. It is, however, too difficult to determine them at the liquid–foam interface directly. Such attention has not been paid in previous works. To determine the adsorption density of the objective substance on bubble surface

[1] To whom correspondence should be addressed.

0021-9797/00 $35.00
Copyright © 2000 by Academic Press
All rights of reproduction in any form reserved.

more exactly, the authors focused on the mass balance at the liquid–foam interface because the liquid–foam interface could be made to correspond to the bottom of the foam bed and the top of the dispersed bubble bed. In this study, the authors performed foam separation of soluble proteins using ovalbumin and hemoglobin at various pH values and determined the liquid flow rate and the protein concentration at the liquid–foam interface by extrapolation based on axial profiles. The aim of this study is to clarify the adsorption of protein onto the bubble surface and its enrichment mechanism in foam separation. The applicability of the Langmuir isotherm of the present system to the adsorption of proteins on the bubble surface will be discussed.

MASS BALANCE EXPRESSION

Figure 1 shows the mass balance for continuous foam separation. Assuming that protein contained in the foam at the liquid–foam interface originates from the adsorbed substance on the bubble surface and from the entrained bulk liquid, the mass balance under a steady state will be expressed by the relation

$$W_{f0}C_{f0} = S_{f0}X + W_{f0}C_b, \quad [2]$$

where C_b and C_{f0} represent the concentration of the protein in the bulk liquid and that in the foam at the interface, respectively. W_{f0} represents the volumetric flow rate of liquid in the foam at the liquid–foam interface, and S_{f0} and X denote the bubble surface area in the foam at the interface and the adsorption density on the bubble surface, respectively. In the foam bed, in general, W_{f0} and S_{f0} decrease, and C_{f0} increases with the increase in foam height because of coalescence of foam cells and liquid drainage. Equation [2] enables us to obtain X if the values of W_{f0}, C_{f0}, and S_{f0} are given or measured. Among these variables, S_f at a definite height in the foam layer is difficult to measure, whereas the surface area of bubbles rising through the column per unit time, S_b, can be estimated from an equation related to the gas holdup and the liquid properties as described later. Assuming that at the liquid–foam interface S_b is equal to S_{f0}, Eq. [2] is rewritten as

$$W_{f0}C_{f0} = S_bX + W_{f0}C_b. \quad [3]$$

Equation [3] gives the relationship between X and C_b and an experimental adsorption isotherm. In this work, C_{f0} and W_{f0} were measured indirectly by an extrapolating method described in the section below. S_b was determined from the relationship proposed by Suzuki *et al*. (17),

$$S_b = 6A\varepsilon(1-\varepsilon)^{4.65}\{(4/225)(\rho_L - \rho_G)^2 g^2/(\mu_L\rho_L)\}^{1/3}, \quad [4]$$

where A, ε, g, ρ_L, ρ_G, and μ_L denote the cross-sectional area of the column, the gas holdup, the gravitational acceleration, the density of liquid and gas, and the viscosity of the liquid, respectively. This equation was derived from the assumption that bubbles are homogeneous spheres whose terminal rising velocity can be calculated by Allen's equation (18), and Shirai's equation (19) was employed for voidage compensation.

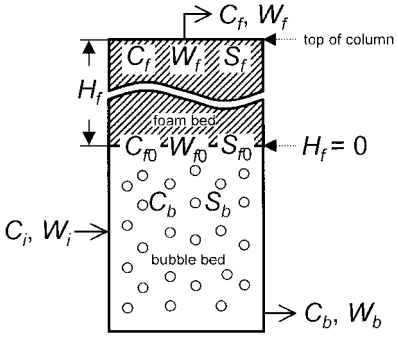


FIG. 1. Schematic diagram of mass balance between the bubble dispersed and the foam bed in the column.

MATERIALS AND METHODS

Materials

Ovalbumin (egg white) was purchased from Eastman Kodak Company or Difco Laboratories. Hemoglobin from bovines was purchased from Wako Pure Chemical Industries Ltd. (Japan). These were used without further purification. The ion strength and pH of their solutions were adjusted with NaCl at 5×10^{-3} M and with aqueous HCl or NaOH to several desired values. All experiments were carried out at room temperature and under atmospheric pressure.

Experimental Setup

The experimental setup used in this study is shown in Fig. 2. The column was constructed of a transparent acrylic resin tube of 4.4×10^{-2} m inside diameter. The main part of this column was 0.65 m in height and was connected to 0.3-m pipes with a flange in order to vary the column height up to 1.25 m. A column of 0.95 m was normally employed, but columns of 0.65 and 1.25 m were also used when necessary. A sintered glass filter with average pore size from 10×10^{-6} to 15×10^{-6} m was installed as a gas distributor at the bottom of the column. Nitrogen gas was supplied to the column through the distributor. In the experiments, a foam collector was equipped at the top of the column to entrap foam generated from the liquid surface. The collector was also made of an acrylic resin cylinder 4.8×10^{-2} m in height and 5.0×10^{-2} m in inside diameter, which corresponded to the outside diameter of the column, with a steel mesh at the bottom end. The collector, filled with a certain amount of polyester fiber wool, was placed at the column top. Pressure taps for measuring gas holdup in the column were installed along the wall at intervals of 0.25 m.

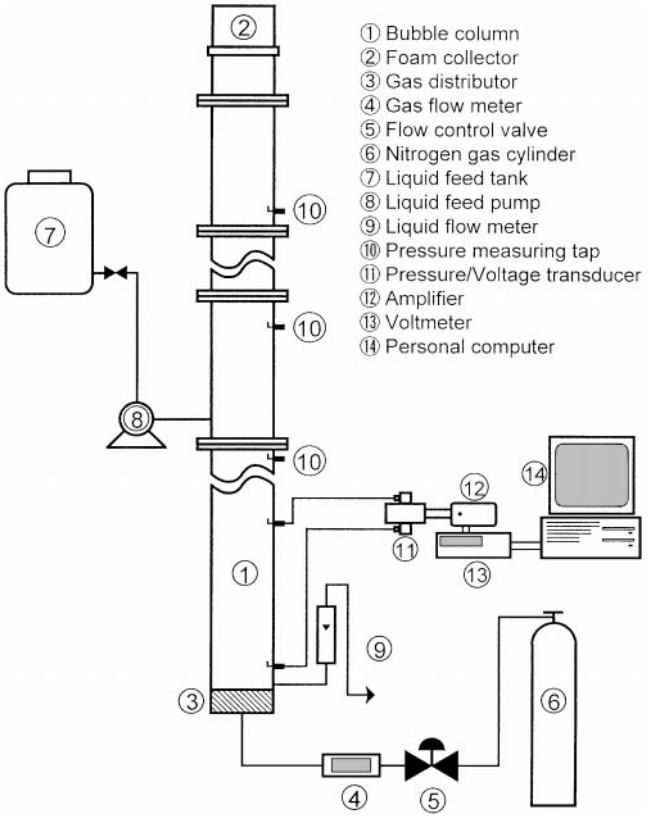


FIG. 2. Schematic drawing of experimental setup for continuous foam separation.

Experimental Procedure for Continuous Foam Separation

Egg ovalbumin (OA) and hemoglobin from bovine (HB) were used as typical water-soluble proteins. Protein solutions prepared at desired concentrations were stored in storage tanks. The solutions were charged into the column from a feed tap by a pump. The volumetric flow rate of feed liquid was 5.0×10^{-7} m^3/s. After the column was filled with the solution, nitrogen gas was supplied and was dispersed as bubbles by the distributor. The foam height, H_f, within the column, that is, the distance between the liquid–foam interface and the column top, was adjusted by control of the volumetric flow rate of the drain liquid using a rotameter. The bulk liquid in the column was regarded as completely mixed because an axial distribution of the bulk concentration was not observed. Thus, it was sampled at the bottom of the column. After steady state was attained after about 2 h, sampling of the foam liquid for measuring the volumetric flow rates and the concentrations was started. The concentrations of the proteins were measured by the Lowry method. The pH of the bulk liquid in the column was measured with a pH meter (ORION Model SA 520). The gas holdup was determined from the difference in static pressure between the clear and aerated liquids using a differential pressure transducer. Voltage signals were recorded by a personal computer (NEC PC-9801 VM) via A/D convertor (CONTEC).

Procedure for Measurement of Axial Profiles of Volumetric Flow Rate of Liquid in Foam

The volumetric flow rate of liquid in the foam was measured as follows. The collector was attached on the top of the column and was exposed to the upward flow of foam generated from the liquid surface. After ca. 15 s, the collector was detached from the column and was weighed on a balance. This procedure was repeated five times using five collectors (for ca. 6 min). The volumetric flow rate, W_f, of liquid in the foam was determined from the change in the sum of the weight of the collectors and the exposure time, assuming that the density of the liquid in the foam was nearly equal to that of water. After the height between the bottom of the foam collector and the liquid–foam interface, H_f, was changed, the experiments were repeated.

RESULTS AND DISCUSSION

Measurement of Volumetric Flow Rate of Liquid in Foam

Typical results of the liquid flow rate in foam layers measured at various H_f are shown in Fig. 3. M in the y axis denotes the value of the cumulative liquid weight of the foam captured by five foam collectors. The relationship between M and the sampling time showed linearity. Therefore, the volumetric flow rate, W_f of liquid in the foam at H_f can be determined from the slope of the plot of M versus sampling time. Other experimental results with different experimental conditions gave the same results as Fig. 3. The solid lines in Fig. 3 are determined by least-squares regression.

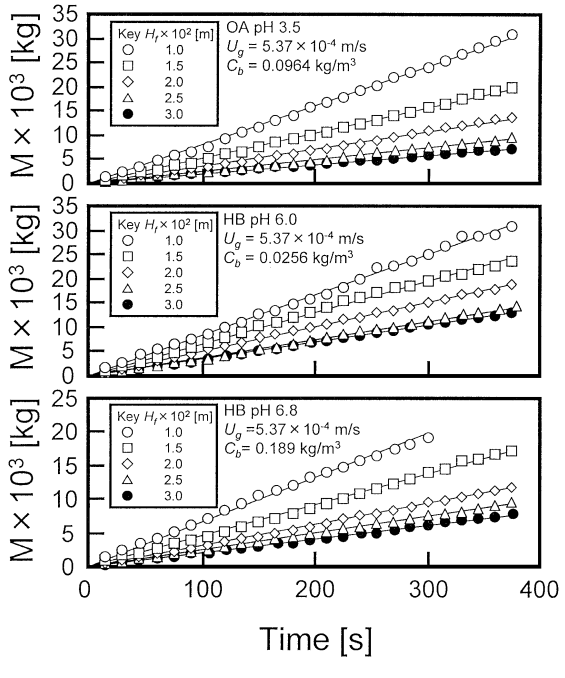


FIG. 3. Typical results of determination of volumetric flow rate, W_f, of liquid in foam at H_f.

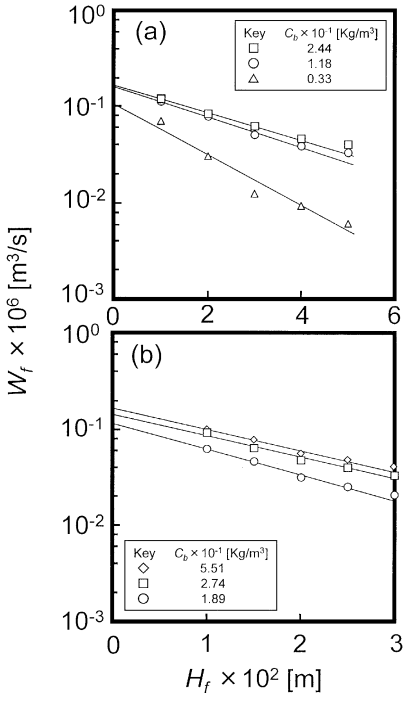


FIG. 4. Axial profiles of the volumetric flow rate of liquid in foam for various bulk concentrations of ovalbumin at pH 4.6 (a) and hemoglobin at pH 6.8 (b). Experiments were conducted with a superficial gas velocity, $U_g = 5.37 \times 10^{-4}$ m/s.

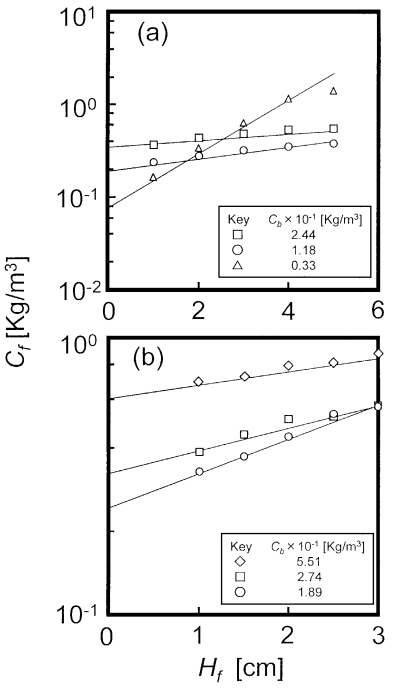


FIG. 5. Axial profiles of the protein concentration in liquid in foam for various bulk concentrations of ovalbumin at pH 4.6 (a) and hemoglobin at pH 6.8 (b). Experiments were conducted with a superficial gas velocity, $U_g = 5.37 \times 10^{-4}$ m/s.

Axial Proiles of W_f and C_f in the Foam Bed

Thus, W_f and C_f at each sampling H_f were obtained in the manner described above and by the Lowry method, respectively. Figures 4 and 5 show typical examples of the axial profiles of the volumetric flow rate, W_f, and the protein concentration, C_f, of liquid in the foam bed for both OA and HB in semi-log plots. W_f was determined from the slope of the plot of M versus sampling time. When H_f increased, W_f decreased and C_f increased exponentially, due to the liquid drainage. The results obtained under different conditions were also similar to these figures. When W_f decreased exponentially, on the other hand, C_f increased exponentially with H_f for both OA and HB. Plots of the logarithms of W_f and C_f versus H_f yielded straight lines with negative and positive slopes, respectively. The intrinsic values of volumetric flow rate, W_{f0}, and protein concentration, C_{f0}, at the liquid-foam interface were determined by an extrapolation method (intercepts of the ordinates both W_f and C_f) as same as the method reported previously for nonfoaming adsorptive bubble separation (18).

Axial Profile of Mass Flux of Proteins in the Foam Bed

Figure 6 shows the axial profiles of the mass fluxes, n_{OA} and n_{HB}, of (a) OA and (b) HB, respectively, as a typical example. Figure 6 depicts the axial distribution of the mass flux of proteins present in the foam. Most of the mass flux in Fig. 6 decreased with increasing H_f. This shows that the liquid drainage occurred due to gravitational acceleration. From a comparison with the results of the axial profiles of W_f and C_f (Figs. 4 and 5), it

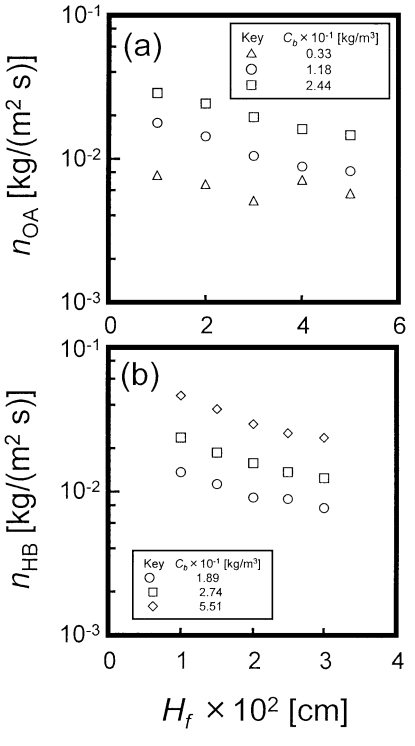


FIG. 6. Axial profiles of the mass flux, n, of proteins for both (a) ovalbumin and (b) hemoglobin in the foam bed. Experiments were conducted with a superficial gas velocity, $U_g = 5.37 \times 10^{-4}$ m/s.

seemed that the mass flux was significantly more influenced by W_f than by C_f. No remarkable coalescence of bubbles within the foam was observed visually under the present experimental conditions along with the foam height. Especially in the case of $C_b = 3.30 \times 10^{-2}$ kg/m^3 for OA, a significant distribution was not observed although the plot shows some scattering. Under this condition, a more "dry" and "cellular" foam was made and the liquid drainage and the collapse of foam cells might be much less for $C_b > 3.30 \times 10^{-2}$ kg/m^3 for OA. The change in the mass flux was influenced by the foam stability as a function of the liquid properties and the operating variables. We will not discuss these influences in any further detail. These axial distributions support the validity of the proposed method for the determination of W_{f0} and C_{f0}. Coalescence of the foam cells would affect the present extrapolation method for the determination of W_{f0} and C_{f0}. If more significant coalescences occurred in the foam bed, the profile of n values should decrease with increasing foam height. This resulted in underestimation of the values of W_{f0} and C_{f0}. The extrapolation method sould be applied to the lower foam height region within the column to avoid underestimation because there was little coalescence in the lower foam height.

Determination of Adsorption Equilibrium Constant and Saturated Adsorption Density

Using Eqs. [3] and [4] and the extrapolated data of W_{f0} and C_{f0} as previously determined in each run, the adsorption isotherms for OA and HB were obtained as shown in Fig. 5. Langmuir's adsorption isotherm, which is well-known, can be expressed as

$$X = K\gamma C_b/(1 + KC_b), \qquad [5]$$

where K and γ denote the equilibrium constant and the saturated surface density on the bubble surface, respectively. The elimination of X from Eqs. [3] and [5] gives

$$W_{f0}(C_{f0} - C_b) = S_b K\gamma C_b/(1 + KC_b). \qquad [6]$$

The reciprocal of Eq. [6] is written as

$$S_b/\{W_{f0}(C_{f0} - C_b)\} = (1/K\gamma)(1/C_b) + 1/\gamma. \qquad [7]$$

Equation [7] is a modified form of the Langmuir adsorption isotherm for the present system. The slope and the intercept of the straight line give the values of K and γ, respectively. S_b, W_{f0}, and C_{f0} have already been estimated; therefore, we can now plot Eq. [7] for both OA and HB as shown in Fig. 7. The straight lines were obtained using the least-squares method. Judging from the fact that the data for both OA and HB are in good accordance with Eq. [7], the adsorption of OA and HB on the bubble surface in a continuous foam separation system should be expressed by Langmuir's isotherm. From the intercept and the slope of each line, the equilibrium constant, K, and the saturated surface density, γ, were obtained for OA and HB as listed in Table 1. The variation of K and γ with pH is shown in panels (a) and (b)

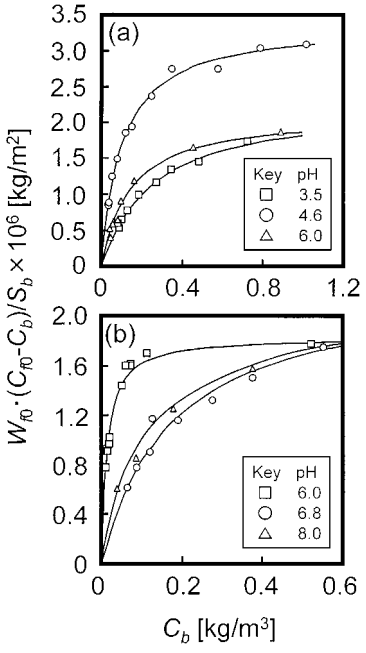


FIG. 7. Adsorption isotherms of (a) ovalbumin and (b) hemoglobin at various pHs. Solid lines in this figure are calculated using K and γ determined from Eq. [7].

of Fig. 7, respectively. The γ values for both OA and HB showed maxima at their respective isoelectric points (i.e.p., pH 4.6 for OA and pH 6.8 for HB) and decreased in the more acidic and alkaline pH regions. On the other hand, K showed a different tendency between OA and HB as is seen in Fig. 7b. K should be strongly influenced by some physicochemical properties such as the hydrophobic characteristics of the protein molecules; thus, the physical meaning of K is more complicated than that of γ. In the following part, some discussion will be given only for γ.

Calculation of Occupied Area for OA and HB on the Bubble Surface in the Saturated State

Assuming that the cross-section of the OA and HB molecules is circular and that they adsorb on the bubble surface in a closest-packing structure (packing fraction = 0.907) in the saturated state, the diameter, D, of the molecules can be calculated from

TABLE 1
Adsorption Parameters for Ovalbumin and Hemoglobin at Various Values of pH

	pH	$\gamma \times 10^6$ [kg/m^2]	$K \times 10^2$ [m^3/kg]
OA	3.5	2.30	3.94
	4.6	3.39	10.1
	6.0	1.92	8.72
HB	6.0	1.96	65.2
	6.8	2.27	5.88
	8.0	1.78	12.7

TABLE 2
Sphere Equivalent Diameters for Ovalbumin and Hemoglobin at Saturated State

	pH	D [Å]
OA	3.5	61.2
	4.6	50.4
	6.0	67.0
HB	6.0	81.6
	6.8	75.8
	8.0	83.6

γ as

$$D = 2\{0.907 M_w/(\pi L \gamma)\}^{0.5}, \quad [8]$$

where L and M_w represent Avogadro's number and the molecular weight of the protein, respectively. The D values of OA and HB were calculated using 45,000 and 65,000 as the M_w for OA and HB, respectively. The diameters obtained at several pHs are listed in Table 2. On the other hand, it is reported that a native OA molecule in an aqueous system is almost spherical with diameter ca. 50 Å based on small-angle X-ray scattering (SAXS) measurement (21). Stein *et al*. (22) reported ovalbumin whose crystal-structure dimensions were $70 \times 45 \times 50$ Å. A vertebrate hemoglobin was said to be a globular protein with dimensions about $64 \times 55 \times 50$ Å (23). It was reported that the dimensions of a hydrated molecule of horse hemoglobin as revealed from its crystal structure analysis were about $70 \times 55 \times 55$ Å (24). Thus, it should be considered that the OA and HB molecules had a closest-packed structure in the saturated state. From a comparison of the D values calculated in this study and the literature data, although D of HB is slightly larger than the literature values, the values for both OA and HB were quite similar to the literature values. This result supports the validity of the proposed method for the determination of the adsorption density in this study.

An electrostatic repulsive force and the van der Waals attractive force act between proteins adsorbed on the air–liquid interface (25, 26). The van der Waals attractive force includes the Hamaker constant, which is a complicated factor. To simplify the discussion, we now focus on the electrostatic repulsive force. The protein molecule is a well-known amphometric macromolecule. The surface charge of the protein molecule originates from the dissociation of the amino acid residues. Tanford *et al.* (27) and Scatchard *et al*. (28) developed the charge model and evaluated the net charge on BSA from the model. We applied the simplified model to both OA and HB. Assuming that the dominant amino acid residues are the carboxyl, amino, imidasol, phenolic hydroxyl, guanidine, and thiol, the dissociation equilibrium constants between these functional groups and a proton are given by

$$K_c = [\text{P–COO}^-]_s[\text{H}^+]_s/[\text{P–COOH}]_s, \quad [9]$$

$$K_p = [\text{P–O}^-]_s[\text{H}^+]_s/[\text{P–OH}]_s, \quad [10]$$

$$K_t = [\text{P–S}^-]_s[\text{H}^+]_s/[\text{P–SH}]_s, \quad [11]$$

$$K_a = [\text{P–NH}_2]_s[\text{H}^+]_s/[\text{P–NH}_3^+]_s, \quad [12]$$

$$K_g = [\text{P–NH}]_s[\text{H}^+]_s/[\text{P–NH}_2^+]_s, \quad [13]$$

$$K_i = [\text{P–N}]_s[\text{H}^+]_s/[\text{P–NH}^+]_s, \quad [14]$$

where $[H^+]_s$ denotes the surface hydrogen ion concentration. Subscripts c, p, t, a, g, and i express the carboxyl, phenolic hydroxyl, thiol, animo, guanidine, and imidasol, respectively. The dissociation degree of each amino acid residue, α, can be written as follows from Eqs. [9]–[14]:

$$\alpha_c = K_c/(K_c + [\text{H}^+]_s), \quad [15]$$

$$\alpha_p = K_p/(K_p + [\text{H}^+]_s), \quad [16]$$

$$\alpha_t = K_t/(K_t + [\text{H}^+]_s), \quad [17]$$

$$\alpha_a = K_a/(K_a + [\text{H}^+]_s), \quad [18]$$

$$\alpha_g = K_g/(K_g + [\text{H}^+]_s), \quad [19]$$

$$\alpha_i = K_i/(K_i + [\text{H}^+]_s). \quad [20]$$

The net charge per protein molecule, z, can be calculated using the following equation:

$$z = (1-\alpha_a)N_a + (1-\alpha_g)N_g + (1-\alpha_c)N_c - \alpha_i N_i - \alpha_p N_p - \alpha_t N_t. \quad [21]$$

In Eq. [21], N denotes the number of each animo acid residue. Figure 10 shows the variation in z with the pH value for both OA and HB. The number of each amino acid residue and the dissociation constants using the calculation of z are summarized in Table 3. In this calculation, the surface concentration of the proton is approximated by its bulk concentration for simplification. The calculated z values for both OA and HB vary from positive to negative with increasing pH and become zero near each i.e.p. The curves for both OA and HB suggest that the electrostatic repulsion is weakest at the i.e.p. and becomes stronger as pH varies from the i.e.p. to the more acidic or alkaline regions. Because

TABLE 3
Type and Number of Amino Acids on OA and HB Using Eq. [21]

	Number (N)		pK	
Type	OA[a]	HB[b]	OA[a]	HB[b]
β,γ-Carboxyl	51	64	3.98	4.00
Imidasole	5	35	5.91	5.90
ε-Amino	22	46	10.51	10.50
Phenolic	10	10	9.95	9.95
Guanidine	14	14	12.00	12.00
Thiol	4	2	8.50	8.50

[a] Refs. (29–32).
[b] Ref. (30).

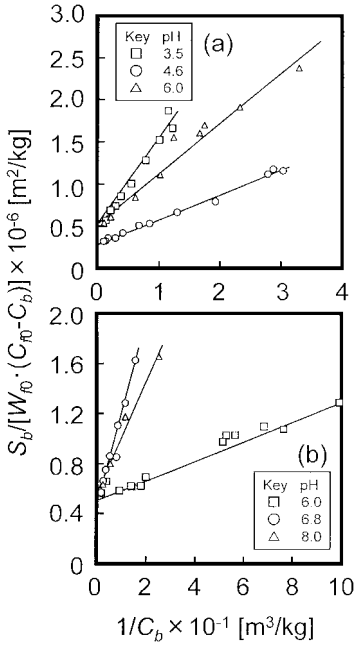


FIG. 8. Estimation of the equilibrium constant and the saturated surface density of (a) ovalbumin and (b) hemoglobin at various pH values by fitting of data to Eq. [7]. Symbols are the same as FIG. 7.

the lateral electrostatic repulsion between protein molecules adsorbed on the bubble surface is considered to be weakest at the i.e.p., therefore negligible, then the proteins are expected to be adsorbed more compactly on the bubble surface and the γ values for both OA and HB show a maximum value at the i.e.p. In the acidic or alkaline pH region, proteins would not be able to be attracted to each other due to the stronger lateral electrostatic repulsion.

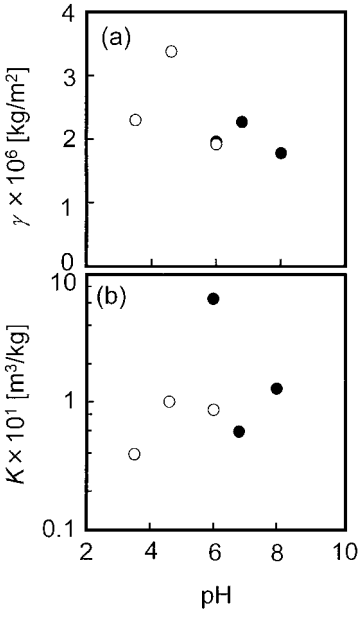


FIG. 9. pH dependence of (a) the saturated surface density, γ, and (b) the equilibrium constant, K, for ovalbumin (○) and hemoglobin (●).

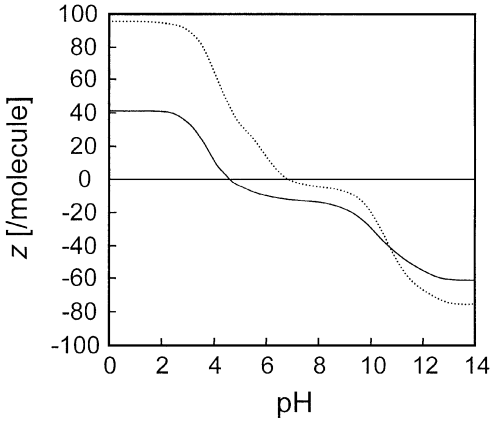


FIG. 10. Variation in the net charge of protein molecule with pH for both ovalbumin (OA) and hemoglobin (HB) calculated by Eq. [21]. Solid and dotted lines correspond to OA and HB, respectively.

CONCLUSIONS

The mechanism of protein enrichment in a continuous foam separation was studied. The experiments were conducted with a bubble column using ovalbumin (OA) and hemoglobin (HB) in various pH ranges as typical water-soluble proteins. Using foam collectors, the volumetric flow rate, W_f, and the protein concentration, C_f, in the foam layer at various heights were measured. The data were processed by the extrapolation method to yield the intrinsic values of W_{f0} and C_{f0} at the interface between the liquid pool and the foam layer. Using the intrinsic values, the adsorption density was determined from the mass balance of protein at the liquid–foam interface. The adsorption isotherms of both OA and HB thus obtained were in good accordance with the Langmuir equation. The two adsorption parameters, the equilibrium constant, K, and the saturated surface density on the bubble surface, γ, were determined from the Langmuir plots modified for the present system. γ for each protein had a maximum value at the i.e.p.; on the other hand, K for OA and HB showed a maximum and a minimum at each i.e.p. The sphere equivalent diameters of OA and HB at several pHs were calculated from the γ values, based on the assumption that proteins at the saturated adsorption state take a two-dimensional closest-packing structure on the bubble surface. The obtained diameters for OA and HB were in good accordance with the literature values. This result supports the validity of the proposed extrapolating method. The reason for the maximum value of γ and the minimum value of occupied area of both OA and HB at each i.e.p. was considered to be qualitatively related to lateral electrostatic repulsion based on the variation of the net charge of the protein molecule with pH calculated from the simplified net charge model.

ACKNOWLEDGMENTS

The authors gratefully acknowledge financial support provided by the Grant-in-Aids for Encouragement of Young Scientists (No. 06760184, 1993), the Minisry of Education, Science and Culture, Japan. The authors thank K. Shirahama, K. Ranba, and S. Shibata, former students of the Department of Chemistry, Hokkaido University, for their help in the experiments. The authors thank

Dr. Isamu Kashiki, Department of Fisheries Oceanography and Marine Science, Hokkaido University, for his suggestions and discussions.

APPENDIX 1

Nomenclature

A a cross-sectional area of bubble column [cm^2]
C_b protein concentrations of the liquids in bulk phase [kg/m^3]
C_f concentrations of the liquids in foam [kg/m^3]
C_{f0} the intrinsic concentration of liquid in foam at the liquid–foam interface [kg/m^3]
C_i concentrations of the feed liquid [kg/m^3]
D sphere equivalent diameters calculated from Eq. [7] [m]
g gravitational acceleration [kg m/s^2]
H_f foam height within column [m]
K equilibrium constant [m^3/kg]
L Avogadro's number [-]
M the value of the cumulative weight of the liquid in foam [kg]
M_w molecular weight [kg/mol]
n mass flux in foam bed [$kg/(cm^2\ s)$]
N number of amino acid residue [/molecule]
S_b production rate of bubble surface area [m^2/s]
S_f bubble surface area in foam at H_f [m^2/s]
S_{f0} bubble surface area in foam at the liquid–foam interface [m^2/s]
U_g superficial gas velocity [m/s]
W_f volumetric flow rate of liquid in foam at H_f [m^3/s]
W_{f0} intrinsic volumetric flow rate at the liquid–foam interface [m^3/s]
W_i volumetric flow rate of feed liquid [m^3/s]
X adsorption density on bubble surface [kg/m^2]
z net charge per protein molecule [/molecule]

Greek Letters

α degree of dissociation [-]
ε gas holdup [-]
γ saturated surface density on bubble surface [kg/m^2]
μ viscosity [kg/(m s)]
ρ density [kg/m^3]

Subscripts

G gas phase
L liquid phase
a amino
c carboxyl
g guanidine
i imidasol
p phenolic hydroxyl
s surface
t thiol

REFERENCES

1. Fuerstenau, D. W., and Healy, T. W., *in* "Adsorptive Bubble Separation Techniques" (R. Lemlich, Ed.), p. 91. Academic Press, New York, 1972.
2. Jenkins, D., Scherfig. J., and Eckhoff, D. W., *in* "Adsorptive Bubble Separation Techniques" (R. Lemlich, Ed.), p. 218. Academic Press, New York, 1972.
3. Bhattacharya, P., Ghosal, S. K., and Sen, K., *Sep. Sci. Technol*. **26,** 1279 (1991).
4. Brown, L., G. Narsimhan, G., and Wankat, P. C., *Biotechnol. Bioeng*. **36,** 947 (1990).
5. Mohan, S. B., Smith, L., Kemp, W., and Lyddiatt, A., *J. Inst. Brew*. **98,** 187 (1992).
6. Montero, G. A., Kirchner, T. F., and Tanner, R. D., *Appl. Biochem. Biotechnol*. **39/40,** 467 (1993).
7. Sarkar, P., Bhattacharya, P., Mukerjea, R. N., and Mukerjea, M., *Biotechnol. Bioeng*. **29,** 934 (1987).
8. Kubota, K., Hayashi, S., and Takubo, Y., *Can. J. Chem. Eng*. **57,** 591 (1979).
9. Kubota, K., Hayashi, S. and Tawa, K., *Kagaku Kougaku Ronbunshu* **8,** 571 (1982).
10. Konduru, R., *J. Chem. Eng. Jpn*. **25,** 548 (1992).
11. Konduru, R., *J. Chem. Eng. Jpn*. **25,** 555 (1992).
12. Brunner, C. A., and Lemlich, R., *Ind. Eng. Chem. Fund*. **2,** 297 (1963).
13. Dick, W. L., and Talbot, F. D., *Ind. Eng. Chem. Fund*. **10,** 309 (1971).
14. Shirotsuka, T., and Ishiwata, M., *Kagaku Kougaku* **37,** 397 (1973).
15. Hartland, S., and Barber, A. D., *Trans. Inst. Chem. Eng*. **52,** 43 (1974).
16. Desai, D., and Kumar, R., *Chem. Eng. Sci*. **38,** 1525 (1983).
17. Suzuki, A., Maruyama, H., Seki, H., and Hayashi, T., *J. Chem. Eng. Jpn*. **28,** 115 (1995).
18. Suzuki, A., Maruyama, H., and Seki, H., *J. Chem. Eng. Jpn*. **29,** 794 (1996).
19. Allen, H. S., *Phil. Mag*. **50,** 323 (1900).
20. Shirai, T., "Ryuudou-sou," p. 115. Kagaku-gijyutsu-sha, Kanazawa (1958).
21. Matsumoto, T., and Inoue, H., *J. Colloid Interface Sci*. **160,** 105 (1993).
22. Stein, P. E., Leslie, G. W., Finch, J. T., McLaughlin, D. J., and Carrell, R. W., *Nature* **347,** 99 (1990).
23. Miki, K., *Tanpakushitu Kakusan Kouso* **32,** 460 (1987).
24. Perutz, M. F., Rossmann, M. G., Cullis, A. F., Munirhead, H., Will, G., and North, A. C. T., *Nature* **185,** 416 (1960).
25. Ahmad, S. I., *Sep. Sci*. **10,** 649 (1975).
26. Uraizee, F., and Narsimhan, G., *Sep. Sci*. **30,** 847 (1995).
27. Tanford, C., Swanson, S. A., and Shore, W. S., *J. Am. Chem. Soc*. **77,** 6414 (1955).
28. Scatchard, G., Coleman, J. S., and Shen, A. L., *J. Am. Chem. Soc*. **79,** 12 (1957).
29. Cannan, R. K., Kibrick, A., and Palmer, A. H., *Ann. N.Y. Acad. Sci*. **41,** 243 (1941).
30. "Biochemical Data Book I" (The Japanese Biochemical Society, Ed.), p. 231. Tokyo-Kagaku-Dohjin, Tokyo, 1979.
31. Nisbet, A. D., Saundry, R. H., Moir, A. J. G., Forthergill, L. A., and Fothergill, J. E, *Eur. J. Biochem*. **115,** 225 (1981).
32. McReynolds, L., O'Malley, B. W., Nisbet, A. D., and Forthergill, J. E., *Nature* **273,** 723 (1978).